Optical characterization of fully programmable MEMS diffraction gratings

F. Zamkotsian, B. Timotijevic, R. Lockhart, R. P. Stanley, P. Lanzoni, M. Luetzelschwab, M. Canonica, W. Noell, M. Tormen

Optical characterization of fully programmable MEMS diffraction gratings

F. Zamkotsian,[1,*] B. Timotijevic,[2] R. Lockhart,[3] R. P. Stanley,[2] P. Lanzoni,[1] M. Luetzelschwab,[2] M. Canonica,[4] W. Noell,[3] and M. Tormen[2]

[1]*Laboratoire d'Astrophysique de Marseille- LAM, Université Aix-Marseille & CNRS, UMR7326, 38 rue Frederic Joliot-Curie, 13388, Marseille Cedex 13, France*
[2]*Swiss Centre of Electronics and Microtechnology, Rue Jaquet-Droz 1, Neuchatel, 2002, Switzerland*
[3]*Ecole Polytechnique Fédérale de Lausanne, Rue Jaquet-Droz 1, Neuchatel, 2002, Switzerland*
[4]*Massachusetts Institute of Technology, 77 Massachusetts Avenue, RM 41-317, Cambridge, Massachusetts, USA*
[*]*frederic.zamkotsian@oamp.fr*

Abstract: We have fabricated and characterized fully programmable diffraction gratings consisting of 64 silicon micro-mirrors. The mirrors are 700µm long and 50µm wide with a fill factor of 90%. They are actuated electrostatically and move down by 1.25µm while showing negligible cross-talk and bowing as small as 0.14µm over 700µm. Extinction ratio up to 100 has been achieved by adjusting only 3 adjacent micro-mirrors. The gratings could operate either as light modulators up to 5µm or spectra generators up to 2.5µm.

OCIS codes: (050.1950) Diffraction gratings; (230.3990) Micro-optical devices.

References and links

1. O. Solgaard, F. S. A. Sandejas, and D. M. Bloom, "Deformable grating optical modulator," Opt. Lett. **17**(9), 688–690 (1992).
2. S. D. Senturia, D. R. Day, M. A. Butler, and M. C. Smith, "Programmable diffraction gratings and their uses in displays, spectroscopy, and communications," J. Microlithogr., Microfabr., Microsyst. **4**, 041401 (2005).
3. O. Solgaard, D. Lee, Y. Kyoungsik, U. Krishnamoorthy, K. Li, and J. P. Heritage, "Microoptical phased arrays for spatial and spectral switching," IEEE Commun. Mag. **41**(3), 96–102 (2003).
4. R. Lockhart, M. Tormen, P. Niedermann, T. Overstoltz, A. Hoogerwerf, and R. P. Stanley, "High efficiency MEMS tuneable gratings for external cavity lasers and microspectrometers," in *Proceedings of IEEE/LEOS Conference on Optical MEMS and Nanophotonics* (Freiburg, Germany, 2008), pp. 33–34.
5. G. B. Hocker, "The Polychromator: a MEMS diffraction grating for synthetic spectra," in *Proceedings of the Solid-State Sensor and Actuator Workshop* (Hilton Head Island, USA, 2000), pp. 89–91.
6. F. Zamkotsian, P. Lanzoni, T. Viard, and C. Buisset, "New astronomical instrument using MOEMS-based diffraction programmable gratings," Proc. SPIE **7208**, 72080I, 72080I-12 (2009).
7. D. M. Burns and V. M. Bright, "Development of microelectromechanical variable blaze gratings," Sens. Actuators A Phys. **64**(1), 7–15 (1998).
8. B. Timotijevic, R. Lockhart, R. Stanley, M. Luetzelschwab, F. Zamkotsian, P. Lanzoni, W. Noell, M. Canonica, and M. Tormen, "Microfabrication of optically flat silicon micro-mirrors for fully programmable micro-diffraction gratings," in Proc. Eurosensors XXVI (2012).
9. S. Senturia, "Programmable diffraction gratings and their uses in displays, spectroscopy, and communications," Proc. SPIE **5348**, 1–6 (2004), doi:10.1117/12.523978.
10. J. Trisnadi, C. Carlisle, and R. Monteverde, "Overview and applications of Grating Light Valve based optical write engines for high-speed digital imaging," Proc. SPIE **5348**, 52–64 (2004), doi:10.1117/12.525898.
11. M. I. Younis, *MEMS Linear and Nonlinear Statics and Dynamics* (Springer, 2011).
12. A. Payne, W. DeGroot, R. Monteverde, and D. Amm, "Enabling high data rate imaging applications with Grating Light Valve™ technology," Proc. SPIE **5348**, 76–88 (2004), doi:10.1117/12.525886.

1. Introduction

Programmable MEMS diffraction gratings (PMDG) are used for external cavity lasers, projection displays and in optical communication systems [1,2]. PMDGs are also used for spectroscopic applications because of their potential in tailoring visible and infrared spectra [3–6]. A common configuration to tailor spectra using a PMDG is to first disperse the input broadband light by a fixed grating onto a programmable grating (Fig. 1), which then selects the wavelengths in the output spectrum. The programmable grating consists of several groups

#173969 - $15.00 USD Received 7 Aug 2012; revised 5 Oct 2012; accepted 5 Oct 2012; published 22 Oct 2012

of micro-mirrors (pixels), where every second micro-mirror in a pixel can move vertically by a fixed displacement, while the other micro-mirrors are not movable. If there is no micro-mirror displacement, the pixel functions as a mirror and the reflected wavelength is preserved in the output spectrum. Displacement of the movable micro-mirrors by λ/4, λ being a wavelength of light impinging on the pixel, makes the pixel to function as a diffraction grating, which switches off the wavelength λ in the output spectrum. A fully programmable MEMS diffraction grating (FPMDG), where every micro-mirror can move independently in a range 0 - λ/2, leads to a better control of the intensity for each wavelength in the synthetized spectrum – the intensity can take any value from 0 (micro-mirror λ/4-condition) to the maximum (no micro-mirror displacement).

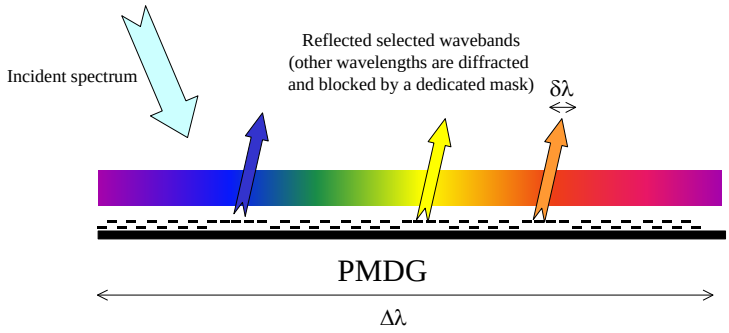

Fig. 1. Principle of wavelengths selection by using a PMDG. Wavelengths wanted in the output spectrum are reflected while the others are diffracted.

One of the main limitations in FPMDG devices is the reduction in diffraction efficiency due to bending of the micro-mirrors during actuation [1]. Burns *et al.* have demonstrated that the diffraction efficiency drops by more than 50% for peak-to-valley micro-mirror bending of λ/4 [7]. In this work we present the optical characterization of microfabricated FPMDG, consisting of 64 independently addressable planar micro-mirrors, showing negligible micro-mirror bending throughout actuation.

2. Design and microfabrication

The FPMDG chip contains 64 micro-mirrors which are actuated electrostatically. Rigid Si micro-mirrors are connected to the centre of the compliant mechanical flexures via linkage arms, as illustrated in Fig. 2.

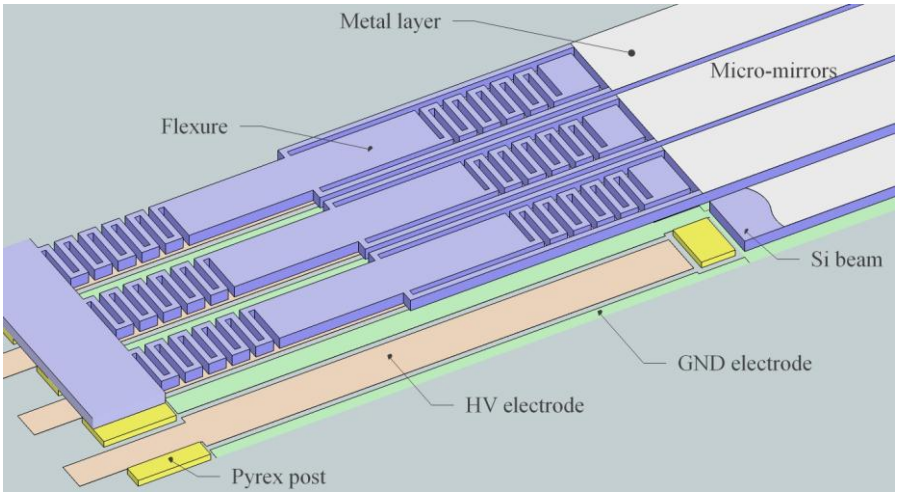

Fig. 2. Schematic of the FPMDG micro-mirrors, flexures and electrodes.

#173969 - $15.00 USD Received 7 Aug 2012; revised 5 Oct 2012; accepted 5 Oct 2012; published 22 Oct 2012

To actuate a micro-mirror, a voltage is applied between the flexures at both ends of the micro-mirror and the underlying electrodes. The electrostatic force pulls the flexures towards the substrate. The mechanical coupling between the optical micro-mirror and the mechanical flexures via the linkage arms permits the micro-mirror to follow the pure vertical displacement of the central point of the flexures, reducing the micro-mirror bending throughout actuation. The micro-mirror and its underlying electrode are kept at ground to eliminate any forces between the mirror and the substrate again reducing stress on the micro-mirror. Flexures and micro-mirrors are made in the same layer (silicon) and are kept at ground through a separate wirebonding connection. The metalized area under the micro-mirrors is also at GND. High-voltage electrodes are present only under the flexures. Grounded metal layer under micro-mirrors is extended between high-voltage electrodes to reduce the cross-talk and micro-mirror bending.

Microfabrication is based on a 4 mask photolithography process [8]. They are used to process an SOI wafer, the device layer of which is used to pattern the micro-mirrors, and a Pyrex wafer, which is used as a chip support with electrodes. The device layer of the SOI wafer is used to pattern optically smooth and low-stress micro-mirrors. Micro-mirror width in the microfabrication process was set to either 50μm or 80μm. The focus in this work is on FPMDG with 50μm wide micro-mirrors as they provide larger diffraction angles, which are easier to resolve by photodetectors.

3. Electro-mechanical characterization

Electro-mechanical characterization of the micro-mirrors is performed with a white light interferometer (WYKO®). The devices were tested using a custom-designed 64channel low-noise voltage source. This source realized in our laboratory exhibits a voltage range from 0 to 150V, a 9.15mV voltage resolution and is controlled by Matlab®.

Micro-mirror bowing has been measured with and without actuation (Fig. 3). In the non-actuated case, a maximum value of 0.14μm has been obtained over the total length of the micro-mirrors (700μm). When actuated, micro-mirror bowing remains unchanged (within 10%) for all possible displacements (up to 1/3 of the vertical gap). The peak-to-valley bowing is less than λ/10 in the IR, demonstrating the validity of the proposed concept to achieve the highest diffraction efficiency.

Similar devices, such as Polychromator [9], show detrimental bending larger than 0.5μm at the micro-mirror edges as a result of non-compensated tensile stress. In the case of GLV [10], the deformation is proportional to the displacement since the micro-mirror is directly actuated by the underlying electrode. As a consequence, the usable optical area reduces as the displacement increases.

#173969 - $15.00 USD Received 7 Aug 2012; revised 5 Oct 2012; accepted 5 Oct 2012; published 22 Oct 2012

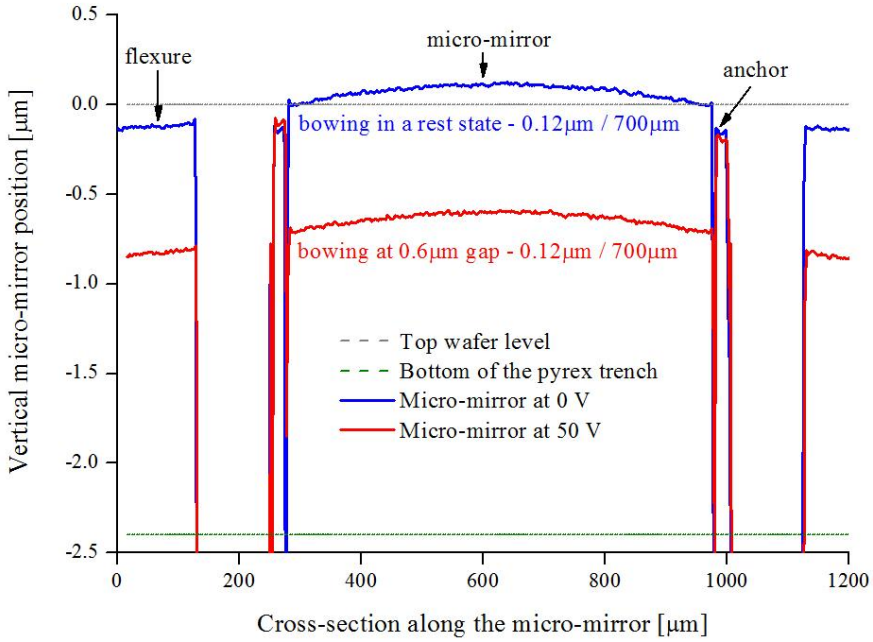

Fig. 3. Bowing of the micro-mirror in the non-actuated state (0 V) and the actuated state (50 V). The initial bowing value of 0.12µm over the micro-mirror length of 700µm remains stable for all possible displacements (up to 1/3 of the vertical gap). In this example the gap is 2.4µm.

The maximum possible displacement is determined by the vertical gap between the micro-mirror and the electrode and is limited to one third of the gap, in order to avoid snap-in of the flexures onto the electrodes [11]. In the current design the gap is kept in the range 2.4-4.2µm, thus, the maximum allowed displacement is 0.8-1.4µm. In the reported experiments a maximum vertical displacement of 1.25µm was achieved without noticing any degradation in the pure piston motion.

The micro-mirror rotation around the short axis (tilt) can significantly degrade the optical performance. On 80µm-chips, a misalignment of roughly 1µm between the micro-mirror and its electrode lead to an unacceptably large tilt, while for 50µm wide mirrors tilt was negligible. Measurements have also confirmed that there is no cross-talk between adjacent actuated and non-actuated mirrors.

4. Optical characterization

The packaged devices have been tested on a dedicated optical bench used for characterizing PMDGs [6]. The input beam, generated with adjustable sources (location, size, spectral type, brightness), is dispersed by a grating and then imaged on the FPMDG, where each elementary wavelength (spectral bin defined by one micro-mirror over the spectral wavelength range dispersed by the fixed grating) is manipulated; the output beam is divided in two parallel spectral and imaging channels for the optical analysis of the tailored signals. In the experiment, the diffracted light from actuated micro-mirrors is filtered out by an output pupil stop (0th order operation) defining the “ON” state along the propagation axis. Measurement of the throughput characteristics of single micro-mirrors at different voltages is made with a point source, around 550nm in wavelength and focused on 2 to 3 micro-mirrors. For spectral tailoring, measurement is done by addressing independently several consecutive micro-mirrors. Schematic of the characterization bench are shown in Fig. 4 featuring the different input and output channels: spectral tailoring could be obtained as described in the introduction. Output channels permit to observe simultaneously image of the input as well as its spectrum.

#173969 - $15.00 USD Received 7 Aug 2012; revised 5 Oct 2012; accepted 5 Oct 2012; published 22 Oct 2012

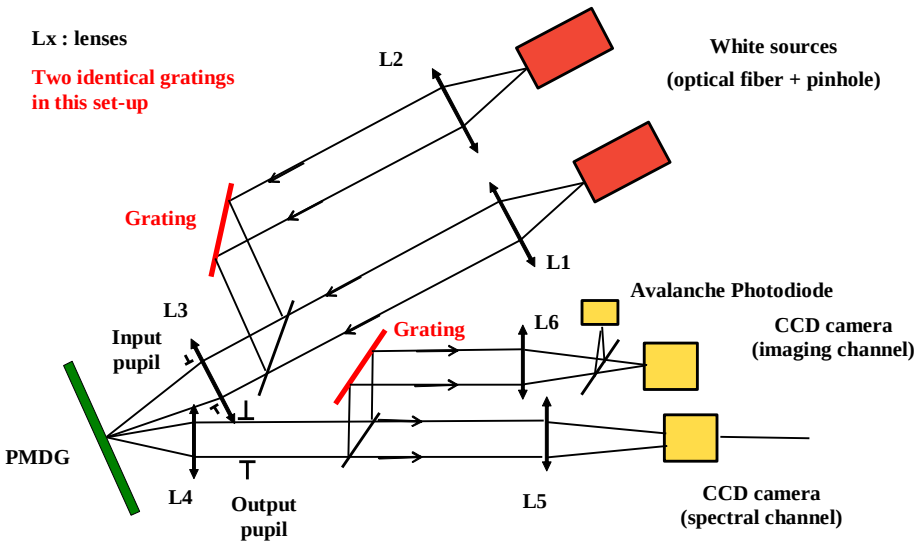

Fig. 4. Schematic of the FPMDG characterization bench.

Figure 5 shows a typical signal coming from the image of the illumination when only one 50µm micro-mirror is actuated electrostatically from 0V to 40V. By increasing the voltage the micro-mirror moves down and the signal is reduced. Once the micromirror has reached the gap of λ/4 at 28V (λ = 546nm), a minimum signal is obtained, equivalent to a π phase shift. By increasing the voltage further, the micro-mirror continues to move downwards, reflecting more light in the 0th order, until it finally reaches the λ/2 condition (equivalent to a 2π phase shift) at 37V, and the signal is fully recovered.

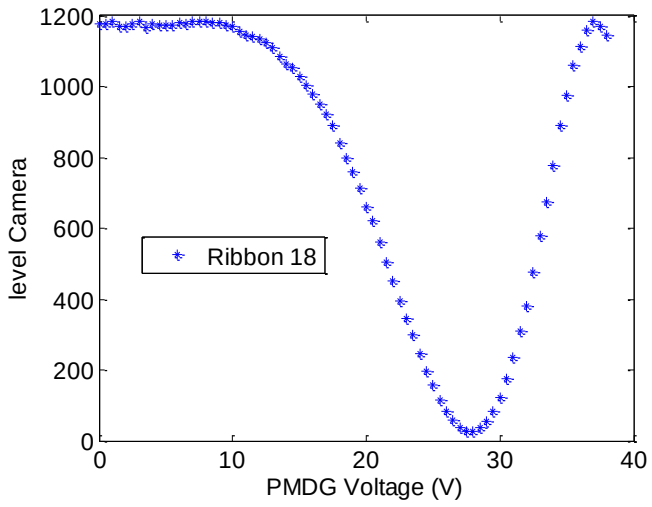

Fig. 5. Optical response when a single micro-mirror is actuated.

When a single micro-mirror is actuated, the highest contrast is reached for the λ/4 condition, and extinction ratios around 20 were obtained for 50µm FPMDG. However, if two or more micro-mirrors are used, the voltages on the micro-mirrors of the FPMDG can be independently adjusted to improve further the extinction ratio. For example, when three micro-mirrors are used, extinction ratios of up to 100 have been achieved. This value is reached by using an iterative process where the voltages of individual micro-mirrors are

#173969 - $15.00 USD Received 7 Aug 2012; revised 5 Oct 2012; accepted 5 Oct 2012; published 22 Oct 2012

scanned between 0V and the voltage needed for reaching λ/4 condition. By minimizing the integrated light on these micro-mirrors; the best group of three voltages is selected and set on the device. A further increase in the number of actuated micro-mirrors does not improve the contrast significantly, meaning that diffraction efficiency maximum of this architecture has been reached.

We have compared the performance of the FPMDG with the performance of GLV device, which is constituted of 1086 "pixels" with 6 ribbons per pixel (3 fixed, 3 variable in Z location). The width of the ribbons is 3.775µm, and the gap width is 0.475µm, leading to a pitch of 4.250µm. The length of the ribbons between two posts is 220 µm. Measured on the same setup, the GLV has shown a maximum contrast of 35, obtained not with 3 consecutive micro-mirrors, but with 6, as imposed by operating conditions: three fixed micro-mirror and three active micro-mirrors at the same voltage. Thus, the FPMDG design gives better performance due to the independent actuation of adjacent micro-mirrors. Moreover, it offers three independently adjustable parameters (voltages) instead of a single one for the GLV.

Generic spectrum generation was tested in the following experiment: a grating disperses a broadband input light on the FPMDG, where 78nm of dispersion is achieved across the field of view. The dispersed light intensity is shown in Fig. 6(a), where the edges and numbers of the micro-mirrors are superimposed. The FPMDG is used to control the intensity of the dispersed spectrum in the different wavelength regions. As an example, 4 sets of micro-mirrors were actuated to reshape the spectrum at 4 spectral positions (Fig. 6(b)), i.e. micro-mirrors 14, 19, 24 and 28 are all biased at 26V; the output dispersed spectrum shows the cancellation of the corresponding wavelengths. The normalized resulting spectrum with respect to the non-actuated spectrum is shown in Fig. 7. At the actuated mirrors location, good extinction is achieved.

In the wavelength proximity of a cancelled wavelength, an excess signal is measured, due to constructive interference effects from diffracted light. One way of understanding this effect is to note that the displaced mirror gives a single slit diffraction pattern which is out of phase with the light reflected from the other mirrors. This effect can be cancelled by small adjustments of the height of the adjacent micro-mirrors.

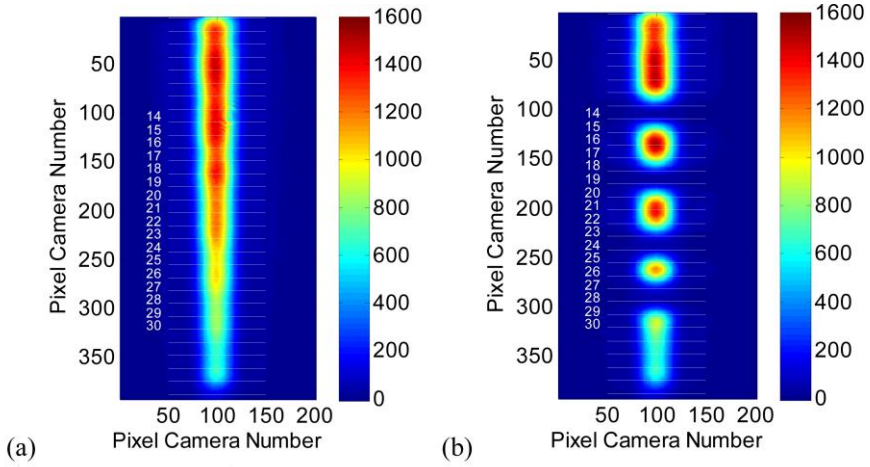

Fig. 6. Input light dispersed (a) over non-actuated FPMDG; (b) over the FPMDG actuated at 4 spectral positions (micro-mirrors 14, 19, 24 and 28 are biased at 26V).

#173969 - $15.00 USD Received 7 Aug 2012; revised 5 Oct 2012; accepted 5 Oct 2012; published 22 Oct 2012

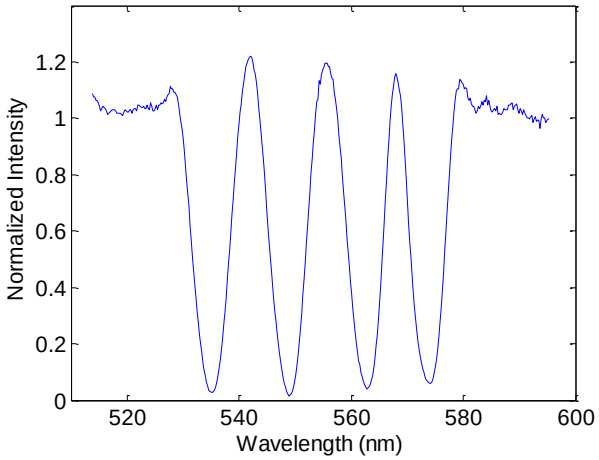

Fig. 7. Spectrum of the input light dispersed over the FPMDG actuated at 4 spectral positions; the response is normalized by the spectral response of non-actuated FPMDG.

FPMDG devices are designed for spectroscopic applications while GLV^{TM} devices are devoted to display images. Therefore, GLV^{TM} components have been designed for reaching very high resonance frequency in the order of 1MHz [6,12] FPMDG are designed to have the first resonant frequency above 10 kHz. The Table 1 summarizes the FEM modelling of the first (out-of-plane) and the second (in-plane) resonant frequencies for fabricated devices.

Table 1. FEM modelling of the first (out-of-plane) and the second (in-plane) resonant frequencies for fabricated devices

Micro-mirror width [µm]	Flexure length [µm]	Number of serpentine meanders	f1 [kHz]	f2 [kHz]
20	340	18	18	21.6
50	415	15	13.7	24

Stability measurement has also been performed. Voltages for λ/4 condition have been applied to 50µm-FPMDG devices and the spectrum evolution has been checked over time. Two sets of measurements have been studied: stability over 4 hours and stability over 12 hours. Photometric measurement reveals a very high stability on actuated micro-mirrors in both cases, within 3% peak-to-valley.

Reproducibility tests have been made by alternating between two patterns: an all-0V pattern and a 3-mirror-deflected pattern where the applied voltages are for the λ/4 condition. Two sets of 32 measurements have been performed for each pattern on the 50 µm FPMDG. Photometric responses of non-actuated (blue curves) and actuated micro-mirrors (red curves) are shown in Fig. 8. In total, 128 curves are superimposed, revealing an excellent reproducibility of the applied pattern. One relevant note is that from the same measurement the crosstalk between micro-mirrors can be evaluated: it is clear that regions of the spectrum that shouldn't be concerned by the actuation of the specific micro-mirrors are effectively not affected, revealing no crosstalk on adjacent micro-mirrors in the measurements.

A similar effect gives rise to a ripple across the entire spectrum (see Fig. 8). This is due to slight differences in micro-mirror position when no voltage is applied. This effect, if necessary, can be compensated through fine adjustment of all micro-mirror voltages, to set all micro-mirrors exactly in the same plane.

#173969 - $15.00 USD Received 7 Aug 2012; revised 5 Oct 2012; accepted 5 Oct 2012; published 22 Oct 2012

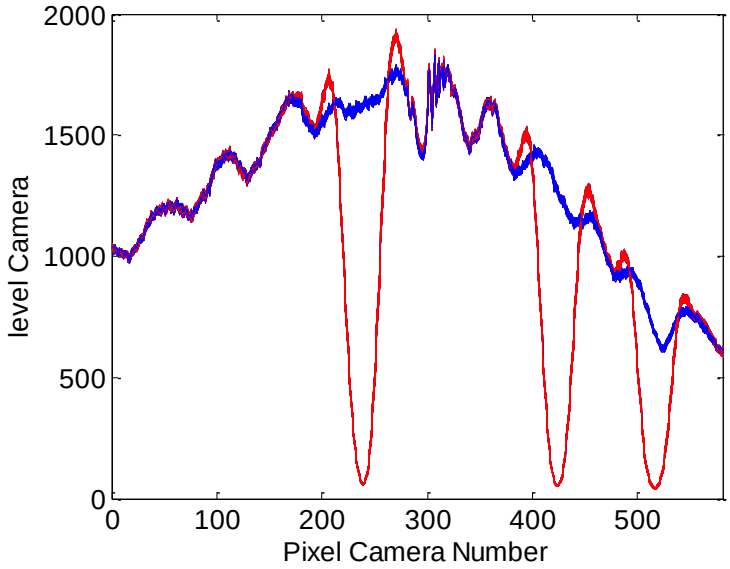

Fig. 8. Reproducibility measurement on the 50µm FPMDG chip; superimposition of all photometric responses obtained with non-actuated micro-mirrors (blue curves) and with three actuated micro-mirrors (red curves) representing four sets of 32 measurements.

5. Conclusion

We have fabricated and characterized a FPMDG with 64 silicon micro-mirrors, with an electrostatically-driven motion of 1.25µm at voltages below 100 V. The micro-mirrors, 50µm and 80µm wide, show negligible cross-talk during the actuation. The micro-mirror bowing is as small as 0.14µm over 700 µm and remains unchanged throughout actuation. Extinction ratios of up to 100 have been achieved by actuating only 3 adjacent micro-mirrors. The measurements have also confirmed a very high stability and good reproducibility over time. Finally, spectral patterns have been successfully generated. Such devices are promising candidates for compact spectroscopic systems as well as scanning and display devices. FPMDG devices with 20µm wide micro-mirrors have also been fabricated and packaged and characterization is under way. Narrower micro-mirrors will provide higher optical performance due to an increased angular separation of the diffraction orders.

Acknowledgments

The authors would like to thank European Space Agency for partly financing the activity "Programmable Micro-Diffraction Gratings" (contract 21212/07/NL/IA) and the ESA technical officer Dr Benedikt Guldimann.

#173969 - $15.00 USD Received 7 Aug 2012; revised 5 Oct 2012; accepted 5 Oct 2012; published 22 Oct 2012